

## Reduction of Enthalpy of Fusion and Anomalies during Phase Transitions in Finely Divided Water

A. Bogdan,<sup>1</sup> M. Kulmala,<sup>1</sup> and N. Avramenko<sup>2</sup>

<sup>1</sup>*Department of Physics, University of Helsinki, P.O. Box 9, FIN-00014 Helsinki, Finland*

<sup>2</sup>*Department of Chemistry, Moscow State University, 119899 Moscow, Russia*

(Received 2 October 1997)

Solid-liquid phase transitions in finely divided water (FDW) obtained by the adsorption of vapor on large silica surface have been studied with differential scanning calorimetry (DSC). Large reduction of both freezing  $\Delta H_f$  and melting  $\Delta H_m$  enthalpies with decreasing the adsorbed weight has been observed. A model for the water/silica system, in which a reduced amount of adsorbed water gives rise to a smaller size of microdroplets, is introduced to explain the reduction of  $\Delta H_f$ ,  $\Delta H_m$ , and other anomalies during the phase transitions in FDW. [S0031-9007(98)06722-2]

PACS numbers: 68.35.Rh

Nanometer-scale materials with their size-dependent physical and chemical properties have received much interest recently [1]. Water, which is certainly the most important liquid on Earth, is of a peculiar character. Thermodynamic properties of bulk water have strong temperature dependence and show extreme anomalies under supercooled conditions [2,3]. But whether its properties depend also on size is still an unresolved problem even though this is of great importance for fundamental and applied interests. This paper concerns the enthalpy of fusion  $\Delta H$  and phase transitions in finely divided water (FDW) with a relatively large free surface.

That the enthalpy of fusion of ice microcrystals may be smaller than that of bulk ice has been proposed long ago [4]. Recently the size dependence of  $\Delta H_m$  was observed for nanometer-scale tin particles by Lai *et al.* [1]. Reduction by 46% in  $\Delta H_m$  was found for a free cluster of 139 sodium atoms [5]. Computational simulation for gold clusters also has shown a reduction in  $\Delta H_m$  [6]. But for FDW the measurements of  $\Delta H_m$  have been done only when it was confined in porous silica glass matrix. In this case, the free surface of liquid was negligibly small, and the role of the matrix was very large. The measurements showed a reduced [7], increased [8], or unchanged [9] value of  $\Delta H_m$ . To the authors' knowledge there are no studies concerning measurements of  $\Delta H_f$  and  $\Delta H_m$  for nanometer-scale water with a large free surface. Theoretical considerations run against the lack of fundamental understanding of the low-temperature behavior of water (the freezing temperature  $T_f$  decreases with size). From the experimental standpoint the problem is that the heat involved in phase transformations of separate particles is rather too miniscule to be measured using existing techniques. Therefore, a "compacted" system of dispersed water, the weight of which would be sufficient to detect the heat evolved, must be used. But a system of nanometer-scale droplets or ice crystals suspended in the unlimited vapor phase or formed on a substrate is in *unstable* equilibrium due to the Kelvin

effect: the larger particles grow at the expense of the smaller ones.

In this Letter we propose a simple method for obtaining FDW with a relatively large free surface and present results of the differential scanning calorimetry (DSC) study of phase transitions in this system. Large reduction in both freezing  $\Delta H_f$  and melting  $\Delta H_m$  enthalpies (J/g) with decreasing the weight of adsorbed water has been observed. Reduction in the bulk temperatures  $T_f$  and  $T_m$ , thermal hysteresis with  $T_f < T_m$ , and "soft" phase transitions have been observed as well. A model in which a reduced amount of adsorbed water gives rise to a smaller size of microdroplets has been introduced to explain the observed phenomena.

DSC is widely used to study phase transitions in condensed matter. Scanning experiments, in which the temperature is changed at a constant rate, are used to determine enthalpies and temperatures of transitions. DSC ensures monotonic cooling and warming, and, therefore, no heat is missed [10]. The amount of material required can be quite small—often less than a milligram.

Compacted systems of FDW were prepared by equilibrating water vapor with a well defined weight of dry fumed silica "S 5380" (product of Sigma), which represents a voluminous powder, particles of which form chain-like aggregates with open networks and large void spaces, as in Fig. 1 [11]. The pans with a thin layer of powder ( $\approx 1.5$  mm) were placed into desiccators where different relative humidities (RH) were maintained. After the equilibrium adsorption has been reached (it could take several days) a well defined weight of the silica/water samples were cold sealed in the standard DSC pans to prevent evaporation. Since annealing for several days at 200 °C before adsorption showed that a negligibly small amount of water was on silica surface, all water on the samples was considered to be owing to adsorption. The amount of the adsorbed water was determined by weighing with accuracy  $\pm 0.1$  mg. The weight of water in the DSC samples was determined by calculation. DSC

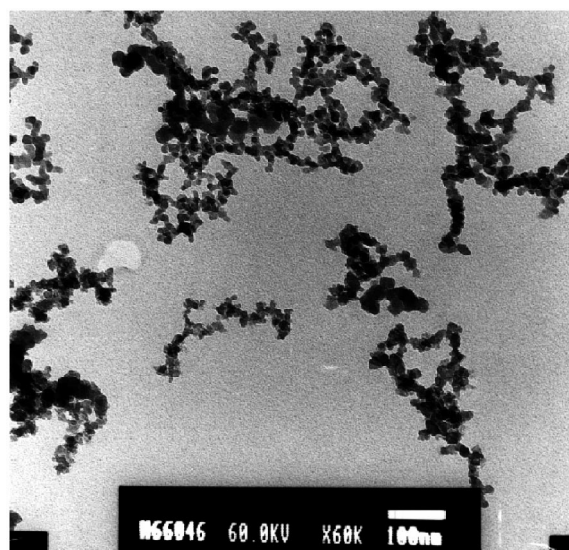


FIG. 1. Fumed silica (surface area  $S = 255 \pm 15 \text{ m}^2/\text{g}$ ). Transmission electron microscopy (TEM).

measurements were carried out with a Mettler DSC-30 (Switzerland) calorimeter. The temperature and energy scales of the DSC were calibrated to the melting temperature of ultrapure indium (99.999%). The accuracy of calibration was  $\pm 0.2 \text{ K}$  for temperature and 2% for enthalpy. The DSC scans were recorded from 200 to 288 K for a scanning rate 3 K/min in cooling and heating modes. Amounts of heat evolved (consumed) during freezing (melting) were reproducible to better than 5%.

How the adsorbed weight decreases with RH is shown in Table I. Formation of FDW and demonstration that a reduced amount of water gives rise to a smaller size water droplets are as follows. Water adsorbs on silanol groups SiOH distributed statistically on the hydrophobic siloxane SiOSi surface [12]. The activation energy for the removal of a water molecule from an isolated SiOH is smaller than from on top of a molecule already adsorbed, i.e., 6 and 10.5 kcal/mol, respectively [12,13]. Thus the adsorbed structure is clustered rather than layered. The fraction of the surface receptive to water is only between 0.15 and 0.25 times its surface area (Plooster and Gitlin [7]). As the adsorption proceeds, the clusters increase and the adjacent ones merge (to reduce the total surface free energy) due to mediation of SiOH between them to form larger liquid regions. At small RH concentration of

molecules in vapor is small, too, and, therefore, size of condensing clusters is smaller than at large RH. Merging events occur more rarely, which leads to the smaller size of liquid regions. Since the void spaces are large (density of fumed silica is very small: water together with the silica itself occupies less than 3% of volume), the liquid-vapor interface is large. All of these allow us to consider the liquid regions as a population of microdroplets. Their size and size distribution depend on the density of SiOH groups, on the geometrical configuration of chains, and on RH. Unfortunately, direct measurements of size of very small water droplets is a very difficult problem because the droplets easily evaporate during the measurements.

The equilibrium of a microdroplet with respect to vapor can be stable if the volume available to it is sufficiently small [4]. Indeed, let the radius of a void space be 90 nm and the radius of a droplet inside it be 10 nm. Then calculations showed that for the variation of droplet radius of only 0.2 nm the changes in vapor pressure which arise from evaporation from (or condensation onto) the droplet is a factor of 3.1, and the changes of vapor pressure resulting from the variation of the droplet radius (Kelvin effect) practically equal zero. Although, the void spaces are interconnected (Fig. 1), the slow exchange of molecules between the voids cannot rapidly equilibrate the abrupt change in pressure if it had occurred suddenly in some void: molecules would be forced to condense (evaporate) immediately.

Results of the DSC measurements are shown in Fig. 2. It is seen that a reduction of  $\text{H}_2\text{O}$  shifts the peaks of the curves towards the low temperature region and decreases the surface area under the DSC signal, which determines the integrated amount of heat evolved (consumed) during transitions. Strongly pronounced thermal hysteresis is clearly seen. Broad maxima in the freezing exotherms demonstrates that heat, contrary to the melting endotherms, evolves stepwise. This together with the asymmetric shape of the curves (at warmer temperatures a larger amount of heat is evolved) confirms that the adsorbed structure is not a continuous film, but rather a population of microdroplets with a wide size distribution. Indeed, if it were layered then there would be no phase transitions because for the given amount adsorbed (Table I) the thickness of the films would be 4, 1.3, and 1 monolayers, respectively. A continuous film is formed only on the *fully hydroxylated* surface, when the number

TABLE I. RH, weight of dry silica, adsorbed weight of  $\text{H}_2\text{O}$ , calculated weights of  $\text{H}_2\text{O}$  in the DSC samples and in HVBL, transition temperatures  $T_f$  and  $T_m$ , experimental  $\Delta H_{f/m}^e$ , corrected  $\Delta H_{f/m}^c$  and bulk  $\Delta H_{f/m}^b$  enthalpies of fusion, radii of ice crystals, and  $r_c$  and  $r_b$ , calculated using  $\Delta H_m^c$  and  $\Delta H_m^b$ , respectively.

RH (%)	Dry $\text{SiO}_2$ (mg)	Ads. $\text{H}_2\text{O}$ (mg)	$\text{H}_2\text{O}$ in DSC (mg)	$\text{H}_2\text{O}$ in HVBL (mg)	$T_f$ ( $^\circ\text{C}$ )	$T_m$ ( $^\circ\text{C}$ )	$\Delta H_{f/m}^e$ (J/g)	$\Delta H_{f/m}^c$ (J/g)	$\Delta H_{f/m}^c$ (J/g)	$\Delta H_m^c$ (J/g)	$\Delta H_{f/m}^b$ (J/g)	$\Delta H_m^b$ (J/g)	$r_c$ (nm)	$r_b$ (nm)
94	2023	626	5.8	0.9	-20.2	-3.2	131.3	149.5	156.6	177.2	288.4	332.2	28.3	15.2
90	1500	152	2.1	1.0	-42.1	-21.4	72.9	79.2	138.2	150.2	209.3	285.6	4.2	2.2
80	1500	113	1.7	1.0	-43.3	-24.8	53.3	54.9	132.8	136.6	197.8	278.2	3.8	1.9

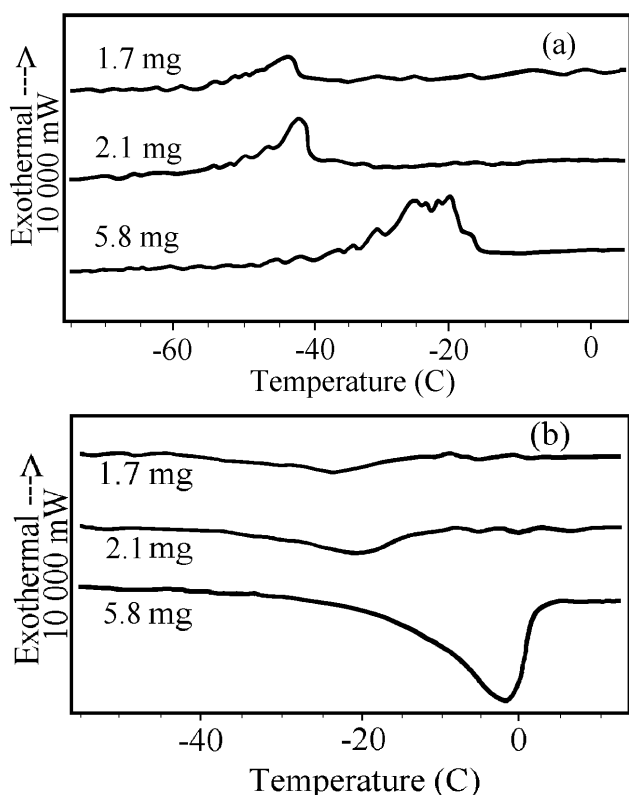


FIG. 2. Effect of the adsorbed weight on the freezing (a) and melting (b) behavior of FDW obtained on fumed silica.

of SiOH per  $\text{nm}^2$  (silanol number) is larger than 5 [12]. In this case strong and highly directional hydrogen bonds between the surface and polar water molecules form a high viscosity boundary layer (HVBL) of up to 3 monolayers [12,14,15] where water remains *unfrozen* even at very low temperature [9,14]. The role of such matrixes on phase transitions in different liquids (including water) has been studied intensively, and the level of understanding is high [10,16]. However, in our case the low density (silanol number  $\approx 2$  [17]) and disordered arrangement of SiOH groups lessen the role of the matrix. HVBL can be formed only on the concave surface, i.e., in the contact points between silica particles, where the density of SiOH groups can be larger.

Depression of  $T_f$  and soft freezing are due to the following two reasons: (i) statistical origin of equilibrium freezing, which states that the probability of density and configuration fluctuations favoring ice formation is larger for larger volumes [2]. If  $N_0$  is the initial number of droplets of volume  $V_d$ , then the number of the unfrozen ones  $N$  is given by [2]

$$N = N_0 \exp\left(-\frac{V_d}{\gamma} \int_T^{T_0} J(T') dT'\right), \quad (1)$$

where  $\gamma = -dT/dt$  is the cooling rate and  $J(T')$  is the ice nucleation rate. The formula shows that supercooling of larger droplets is smaller than that of smaller ones. (ii) The value of the *contact angle for ice* (determined

by the configuration of the surface field, formed by the disordered SiOH groups, and its interaction with water molecules) is greater than zero and has a distribution: the consequence is that heterogeneous freezing occurs at a cooler and broader temperature range. A low-temperature tail is due to the freezing of the smallest drops, and the larger ones formed on the surface with an ordered structure of SiOH. In the latter case the influence of a HVBL is large, and homogeneous freezing starts from outside the HVBL at temperatures lower than  $-40^\circ\text{C}$  [2,16].

Smooth endotherms are due to gradual melting of ice crystals with a wide size distribution. It is known that small crystals melt at lowered temperatures [18,19]. Depression of melting point  $T_m$  is a quasilinear function of crystal radius  $r$  and is given by the Gibbs-Thomson equation [20]

$$T_m = \frac{2\sigma_{iw}T_0}{\rho_i\Delta H r}, \quad (2)$$

where  $\sigma_{iw}$  is ice/water interface energy,  $\rho_i$  is the density of ice, and  $T_0 = 273.15$  K. In equilibrium thermodynamics all parameters entering Eq. (2) assume the well defined quantities which are independent of size. But it does not seem very likely that nanometer-scale particles should possess the macroscopic properties. For instance, recently an assumption has been expressed that the reduction in  $\Delta H$  in small systems may also be responsible for the soft transitions, the width of which depends on  $\Delta H$  [5,21].

Hysteresis between  $T_f$  and  $T_m$  is due to the essential asymmetry between freezing and melting. In the former case an energy barrier must be overcome, i.e., nucleation of the ice phase must occur. In the case of melting an energy barrier is absent or it may be very small. The low thermal conductivity of ice and large latent heat of fusion make melting gradual (in comparison with metal) propagating slowly from the surface into the ice. Therefore, substantial supercooling of water is normal, whereas there is no superheating of ice.

Experimental data and the main thermodynamic features of Fig. 2, listed in Table I, can be summarized as follows: (i) the amount of the adsorbed water decreases with RH; (ii) the peak transition temperatures with  $T_f < T_m$  are far below the bulk melting point and decrease with the weight of water in the DSC samples; (iii) experimental enthalpies,  $\Delta H_{f/m}^e$ , calculated by dividing the integrated amount of heat by the weight of water, decrease as well; and (iv) the values of  $\Delta H_{f/m}^e$  are smaller than the enthalpies of bulk water,  $\Delta H_{f/m}^b$  calculated at  $T_f$  and  $T_m$  according to Eq. (3-26) from [2].

When considering  $\Delta H_f^e$  and  $\Delta H_m^e$  the question arises whether the reduction is actual or is caused by (i) part of the heat was missed; (ii) part of the water evaporated during loading the DSC pans; (iii) part of the water remained unfrozen. It was said above that DSC ensures no heat is missed [10]. The evaporated weight was estimated to be smaller than 3% and smaller for smaller RH. Weight of the unfrozen water in the HVBL was

calculated using surface area of silica and silanol number. For a HVBL with thickness of three monolayers, the weight is  $46 \pm 2.76$  mg per g of silica. This gives a fraction of the unfrozen water 0.15, 0.45, and 0.59 for the samples with 5.8, 2.1, and 1.7 mg of water, respectively. Most likely, this weight of HVBL is overestimation, since our nuclear magnetic resonance (NMR) measurements gave the fraction smaller than 0.05 for the comparable weight of 8.6 mg at  $-60^\circ\text{C}$  [11]. But even subtraction of the unfrozen water gave the corrected values of enthalpies  $\Delta H_f^c$  and  $\Delta H_m^c$  smaller than those of bulk. Accuracies of calculated  $\Delta H_{f/m}^c$  are 7.6%, 14.4%, and 16.3% for the weights of 5.8, 2.1, and 1.7 mg, respectively.

Corrected  $\Delta H_m^c$  and bulk  $\Delta H_m^b$  were used in Eq. (2) for calculation of radii of ice crystals  $r$  corresponding to  $T_m$ . The temperature dependence of  $\sigma_{i/w}$  was taken into account according to Eq. (5-47) from [2]. It is seen from Table I that  $r_c > r_b$ . To find out which of them are physically more reasonable we calculated approximately the fraction of surface covered by water using both sets of radii and compared the results with the experimental data (see above). Since the droplets formed are not spherical and the contact angle for water is  $55^\circ$  [22] (the size of microdroplets is sufficiently large to use this macroscopic parameter), it was assumed that their volume is  $\approx 1/5$  that of the spherical droplet. The fractions calculated using  $r_c$  are 0.18 and 0.22 (for  $r_b$ , 0.41 and 0.45) for the weights 2.1 and 1.7 mg, respectively. The good agreement with the experimental data obtained for  $r_c$  is easy to explain. At low RH microdroplets are formed mainly on the parent SiOH when no rehydration ( $\text{SiOSi} + \text{H}_2\text{O} \rightarrow 2\text{SiOH}$ ) takes place. At large RH rehydration and capillarity condensation lead to increasing the fraction of surface covered with water, which is difficult to calculate. Finally, an interesting finding concerning the  $\Delta H_{f/m}^e$  and  $\Delta H_{f/m}^c$  is that the difference  $\Delta H_m^{e_c} - \Delta H_f^{e_c}$  decreases with decreasing water, as shown in Table I. This is in contrast to the bulk case, when lowering temperature leads to an increase of  $\Delta H_m^b - \Delta H_f^b$ . This behavior may be due to the fact that for very small particles the difference between the specific heats of water and ice becomes smaller.

In summary, in contrast to embedding water in fully hydroxylated matrix, the present method allows us to obtain a system of FDW with relatively large free surface. The samples prepared in such a way are ideal for studies of melting and freezing behavior with DSC, NMR. The reduced  $\Delta H_f$  and  $\Delta H_m$  observed (for the first time) with decreased water adsorbed on silica surface is evident and cannot be explained from the traditional experimental viewpoints. Within the context of the proposed model the experimental data show that smaller water droplets have decreased  $\Delta H_f$  and  $\Delta H_m$  as well as  $T_f$  and  $T_f$ .

The financial support from the Academy of Finland is gratefully acknowledged. We thank J. Augustin for pro-

viding us with the good photograph of silica and I. Ford, A. Laaksonen, and J. Mäkelä for helpful discussions.

- 
- [1] B.E. Wyslouzil *et al.*, Phys. Rev. Lett. **79**, 431 (1997); A. Bogdan, J. Chem. Phys. **106**, 1921 (1997); S.L. Lai *et al.*, Phys. Rev. Lett. **77**, 99 (1996); R.R. Vanfleet and J.M. Mochel, Surf. Sci. **341**, 40 (1995); M. Wautelet, J. Phys. D **24**, 343 (1991).
  - [2] H.R. Pruppacher and J.D. Klett, *Microphysics of Clouds and Precipitation* (Kluwer Academic Publishers, Dordrecht, 1997), Chaps. 3,5,7,9.
  - [3] C.A. Angel, in *Water and Aqueous Solutions at Subzero Temperatures*, edited by F. Franks (Plenum Press, New York and London, 1982), Vol. 7, p. 1.
  - [4] R. Defay and I. Prigogine, *Surface Tension and Adsorption* (Longmans, New York/London, 1966), Chap. 15.
  - [5] M. Schmidt *et al.*, Phys. Rev. Lett. **79**, 99 (1997); G. Bertsch, Science **277**, 1619 (1997).
  - [6] F. Ercolessi, W. Andreoni, and E. Tosatti, Phys. Rev. Lett. **66**, 911 (1991).
  - [7] M.N. Plooster and S.N. Gitlin, J. Phys. Chem. **75**, 3322 (1971); G.G. Litvan, Can. J. Chem. **44**, 2617 (1966).
  - [8] W.A. Patrick and W.A. Kemper, J. Phys. Chem. **42**, 369 (1938).
  - [9] G.K. Rennie and J. Clifford, J. Chem. Soc. F1 **73**, 680 (1977).
  - [10] E. Molz *et al.*, Phys. Rev. B **48**, 5741 (1993).
  - [11] A. Bogdan *et al.*, J. Colloid Interface Sci. **177**, 79 (1996); A. Bogdan and M. Kulmala, J. Colloid Interface Sci. **191**, 95 (1997).
  - [12] R.K. Iler, *The Chemistry of Silica* (Wiley, New York, 1978), Chaps. 5 and 6.
  - [13] K. Klier and A.C. Zettlemoyer, J. Colloid Interface Sci. **58**, 216 (1977).
  - [14] K. Overloop and L. Van Gerven, J. Magn. Reson. A **101**, 179 (1993).
  - [15] D.R. Bassett, E.A. Boucher, and A.C. Zettlemoyer, J. Colloid Interface Sci. **34**, 436 (1970); D.R. Bassett, E.A. Boucher, and A.C. Zettlemoyer, J. Colloid Interface Sci. **27**, 649 (1968).
  - [16] J-C. Li, D.K. Ross, and R.K. Heenan, Phys. Rev. B **48**, 6716 (1993); R. Mu and V.M. Malhotra, Phys. Rev. B **44**, 4296 (1991); J. Warnock, D.D. Awschalom, and M.W. Shafer, Phys. Rev. Lett. **57**, 1753 (1986); J.L. Tell and H.J. Maris, Phys. Rev. B **28**, 5122 (1983).
  - [17] H. Barthel, Colloid Surf. A, Physicochem. Eng. Aspects **101**, 217 (1995).
  - [18] J.H. Bilgram, Phys. Rep. **153**, 1 (1987).
  - [19] M. Wautelet, Eur. J. Phys. **16**, 283 (1995); P.R. Couchman and W.A. Jesser, Nature (London) **269**, 481 (1977); P. Buffat and J-P. Borel, Phys. Rev. A **13**, 2287 (1976).
  - [20] C.L. Jackson and G.B. McKenna, J. Chem. Phys. **93**, 9002 (1990).
  - [21] P. Labastie and R.L. Whetten, Phys. Rev. Lett. **65**, 1567 (1990).
  - [22] Chin-Cheng Chen *et al.*, J. Colloid Interface Sci. **157**, 465 (1993).